

Morphology and Morphometry in Chronic Spinal Cord Injury Assessed Using Diffusion Tensor Imaging and Fuzzy Logic

Benjamin M. Ellingson, John L. Ulmer, Robert W. Prost, and Brian D. Schmit

Abstract—Diffusion tensor imaging (DTI) using a combination of direct anisotropy measurements provided a more anatomically accurate morphological representation of the human spinal cord than traditional anisotropy indices. Furthermore, the use of a fuzzy logic algorithm to segment regions of gray and white matter within the spinal cord based on these anisotropy measurements allowed for morphometric analyses. Results indicated a significant decrease in overall spinal cord cross-sectional area, dorsal funiculus cross-sectional area, and lateral funiculi cross-sectional area in subjects with injury compared to the neurologically intact control subjects. Results also showed individuals with caudal injuries had a morphology and morphometry that was more similar to that of the control subjects, which is consistent with the process of Wallerian degeneration and has been illustrated by previous investigations involving animal surrogates.

Index Terms—Diffusion Tensor Imaging, Spinal Cord Injury, Fuzzy Logic

I. INTRODUCTION

DIFFUSION tensor imaging (DTI) is a promising technique for obtaining anatomically accurate images of the human spinal cord. An accurate anatomical representation of the spinal cord is critical for precise diagnosis and planning of surgical treatment strategies. Traditional magnetic resonance imaging (MRI) gives little information regarding white matter tract integrity [1] and has been shown to give no new information during the acute stages of traumatic spinal cord injury [2]. Diffusion tensor imaging is more sensitive than traditional MRI to the physiological integrity of the spinal cord [3-5], although there are some morphologic inconsistencies in images of internal spinal cord morphology obtained with

traditional diffusion anisotropy indices, primarily in the ventral gray matter regions [6].

DTI uses the diffusion properties of different tissue types to delineate anatomical boundaries. Anisotropic diffusion in the central nervous system is caused barriers to diffusion, such as cell membranes, and previous experimental investigations have shown that anisotropy increases with an increase in axonal fiber density, a decrease in axonal fiber diameter, or a decrease in membrane permeability [7, 8]. Furthermore, diffusion coefficients and mean diffusivity for the spinal cord change significantly in pathological conditions [3, 5], suggesting that these characteristics could be useful in monitoring changes in the spinal cord after injury.

Although diffusion anisotropy indices have been useful for identifying changes in the spinal cord following injury, detailed morphologic quantification is not feasible using current techniques. Morphometric analysis is particularly useful in clinical assessment of conditions such as compression myelopathy [9] and may also give quantitative information regarding the amount of atrophy and degeneration after traumatic spinal cord injury. In a previous investigation we demonstrated the use of fuzzy logic to delineate gray and white matter in the spinal cord using various anisotropy indices [6]. We propose fuzzy logic can also be applied using anisotropy measurements to segment gray and white matter for the use in morphometric analysis following spinal injury.

In the current study, we compared the contrast between gray and white matter, and anatomical representations of the intact human spinal cord using direct measures of anisotropy with similar measurements obtained from traditional DTI indices. We then used these anisotropy measurements to train a fuzzy inference system (FIS) to classify regions of white matter to assess atrophy and degeneration in subjects after traumatic spinal cord injury.

II. METHODS

A. Subjects

Five neurologically intact subjects free from medical implants and five subjects with varying levels of spinal cord injury participated in this study. All procedures were approved by the Institutional Review Boards of Marquette University and the Medical College of Wisconsin.

Manuscript received April 24, 2006.

B. M. Ellingson is with the Department of Biomedical Engineering, Marquette University, Milwaukee, WI 53201 USA. (e-mail: benjamin.ellingson@marquette.edu).

B. D. Schmit is with the Department of Biomedical Engineering, Marquette University, Milwaukee, WI 53201 USA (phone: 414-288-6125; fax: 414-288-7938; e-mail: brian.schmit@marquette.edu).

J. L. Ulmer is with the Department of Radiology, Medical College of Wisconsin, Milwaukee, WI 53226 USA. (e-mail: julmer@mcw.edu).

R. W. Prost is with the Departments of Radiology and Biophysics, Medical College of Wisconsin, Milwaukee, WI 53226 USA. (email: prostr@mcw.edu).

B. MRI

A total of eight axial slices were obtained throughout the upper cervical spine (C1 – C4 determined by localizer images and anatomical references) using a dual spin echo EPI diffusion weighted pulse sequence. A head coil (Head Coil, GE Medical Systems, Waukesha, WI) and 1.5 T clinical MR scanner (GE Horizon, GE Medical Systems, Waukesha, WI) were used to acquire all images. Images were collected with TR/TE/NEX = 6000ms/88.1ms/4, FOV = 20 cm, slice thickness = 5 mm, and slice spacing = 1.5 mm. The acquisition matrix was 256 x 256 and *b*-value was set to 1500 s/mm². The resulting voxel dimensions were 0.78 mm x 0.78 mm x 5 mm. Images were cropped to 100 pixels x 100 pixels for quick analysis and illustrative purposes. Linear regression was used to calculate the diffusion tensor from a total of 25 diffusion weighted images obtained from 25 equidistant diffusion sensitizing gradient directions. All images were saved in DICOM format and analyzed using MATLAB (MathWorks, Natick, MA). The principle eigenvalues (λ_1 , λ_2 , and λ_3 corresponding to the largest to smallest eigenvectors, respectively) were obtained and used in calculation of the anisotropy indices.

C. Anisotropy Measurements and Fuzzy Inference System

Traditional anisotropy indices used in DTI of the spinal cord include the longitudinal apparent diffusion coefficient (lADC), transverse apparent diffusion coefficient (tADC), mean diffusivity (MD), and fractional anisotropy (FA). Anisotropy measurements, defined as deviation of the eigenvalues with respect to the mean diffusivity, were also used in this study. Anisotropy for a particular voxel was defined as

$$\Psi = \begin{bmatrix} \psi_1 \\ \psi_2 \\ \psi_3 \end{bmatrix} = \begin{bmatrix} \lambda_1 - MD \\ \lambda_2 - MD \\ \lambda_3 - MD \end{bmatrix} \quad (1)$$

where ψ_1 is the anisotropy (mm²/s) corresponding to the largest eigenvector, λ_1 is the diffusion (mm²/s) corresponding to the largest eigenvector, and *MD* is the mean diffusivity (mm²/s) defined as the average of the eigenvalues.

Distributions were extracted for gray matter (GM), white matter (WM), and cerebrospinal fluid (CSF) for each of the anisotropy measurements ψ_1 , ψ_2 , and ψ_3 by superimposing a digitized histological template for the C2 level of the spinal cord onto the control subject data. These distributions were used as membership functions for a Mamdani-type fuzzy inference system [10] used for tissue classification. The membership functions represented the degree of membership a particular index value has in a specific region of interest. The process of calculating the degree of membership for a particular index value is termed *fuzzification* and is defined as

$$\mu(\psi) = \begin{bmatrix} \mu_{CSF}(\psi_1) & \mu_{GM}(\psi_1) & \mu_{WM}(\psi_1) \\ \mu_{CSF}(\psi_2) & \mu_{GM}(\psi_2) & \mu_{WM}(\psi_2) \\ \mu_{CSF}(\psi_3) & \mu_{GM}(\psi_3) & \mu_{WM}(\psi_3) \end{bmatrix} \quad (2)$$

where μ is the fuzzification function matrix and

$$\mu_{ROI}(index) = \frac{1}{\sqrt{2\pi s_{index,ROI}}} e^{-\frac{(index-m_{index,ROI})^2}{2 \cdot s_{index,ROI}^2}} \quad (3)$$

is the Gaussian membership function for a specific anisotropy index and region of interest, $m_{index,ROI}$ is the sampled mean value for a particular index and region of interest, and $s_{index,ROI}$ is the sampled standard deviation for a particular index and region of interest obtained using the histological template. To logically determine which region is represented in a particular voxel we apply the *and* logical operation such that

$$\beta = \text{and}(\mu(\chi)) \quad (4)$$

where

$$\text{and}(\mu_{ROI}(\chi)) = \prod_{\in index} \mu_{ROI}(index). \quad (5)$$

The degree of membership of a particular voxel in a particular region of interest was mapped to the output variable space using a set of output membership functions defined in the output membership function matrix,

$$\xi(y) = [\xi_{GM}(y) \quad \xi_{WM}(y) \quad \xi_{CSF}(y)], \quad (6)$$

with individual output membership functions defined as

$$\xi_{GM}(y) = \begin{cases} 2y & \text{for } 0 \leq y \leq 0.5 \\ -2y - 2 & \text{for } 0.5 \leq y \leq 1 \end{cases} \quad (7)$$

$$\xi_{WM}(y) = \begin{cases} 0 & \text{for } 0 \leq y \leq 0.5 \\ 2y - 1 & \text{for } 0.5 \leq y \leq 1 \end{cases} \quad (8)$$

$$\xi_{CSF}(y) = \begin{cases} -2y + 1 & \text{for } 0 \leq y \leq 0.5 \\ 0 & \text{for } 0.5 \leq y \leq 1 \end{cases} \quad (9)$$

The output variable, termed the *fuzzy anisotropy index*, was determined by

$$y = \text{centroid}(\min(\text{and}(\mu_{ROI}(\chi)), \xi_{ROI}(y))\Phi) \quad (10)$$

where $\Phi = [1 \quad 1 \quad 1]'$ is the matrix sum.

D. Area Calculations & Diffusion Measurements

Spinal cord cross-sectional areas were calculated by counting the number of pixels in a particular region of interest for a particular slice and multiplying by the voxel dimensions. The entire cross-sectional area of the spinal cord and cross-sectional area of white matter regions were calculated for each slice and averaged across the respective spinal levels. Differences in cross-sectional areas were compared using a two-way ANOVA comparing the mean area to subject type and spinal level. Significant differences in the ANOVA ($p < 0.05$) were further analyzed using Tukey's method for multiple

comparison testing. The percentage difference in white matter cross-sectional area for subjects with spinal cord injury with respect to the neurologically intact control subjects was calculated to give quantitative insight into the amount of atrophy.

Changes in longitudinal apparent diffusion coefficient (LADC), transverse apparent diffusion coefficient (tADC), mean diffusivity (MD), and longitudinal measured anisotropy (ψ_1) were evaluated in the dorsal columns and lateral funiculi by manually selecting regions of interest on the fractional anisotropy images. Differences in diffusion values were compared using a one-way ANOVA comparing the diffusion and anisotropy measurements in the spinal cord injured subjects to that of the neurologically intact control subjects.

III. RESULTS

Results indicated better anatomical accuracy in anisotropy measurements compared to fractional anisotropy, as illustrated in Fig. 1. The detectability index [11], a measure of contrast between tissue types, quantitatively validated the observed differences ($p < 0.05$).

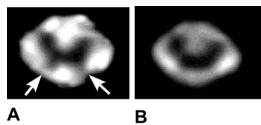


Fig. 1. C1 image of neurologically intact spinal cord. A) Anisotropy measurement showing the presence of the ventral horns of the gray matter (arrows), and B) fractional anisotropy. Images were upsampled 4x and linearly interpolated for illustrative purposes.

The C1 level images of anisotropy measurements and FIS segmented white matter regions for the spinal cord injured subjects and a single neurologically intact control subject are shown in Fig. 2.

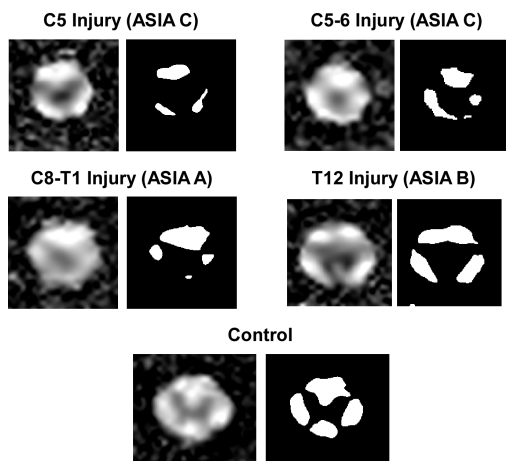


Fig. 2. Anisotropy measurements and FIS segmented white matter regions in spinal cord injured and neurologically intact control subjects at the C1 spinal level (rostral to injury site). Images were upsampled 4x and linearly interpolated for illustrative purposes.

Morphometric analysis comparing neurologically intact control subjects to spinal cord injured subjects indicated a significantly larger ($p < 0.001$) overall cross-sectional area of the upper cervical spinal cord in the control subjects (95 ± 5 s.d. mm 2) compared to all the cervical injured subjects ($60 - 80$ mm 2), with the T12 injured subject closer to the control values (94 ± 8 s.d. mm 2). Cross-sectional area of the total white matter was also significantly higher ($p < 0.001$) in control subjects (45 ± 10 s.d. mm 2) compared to all the cervical injured subjects ($15 - 25$ mm 2), again with the T12 injured subject closer to controls (40 ± 12 s.d. mm 2). ANOVA results also indicated a significant difference between the C3 and C4 levels ($p < 0.01$), indicating the start of the cervical enlargement. The percentage loss of cross-sectional area in specific white matter tracts, calculated with respect to the same regions in the neurologically intact control subjects, indicated a significant decrease in cross-sectional area in all regions of white matter ($p < 0.01$) for all subjects with spinal cord injury, with the left and right funiculi in the C5, C5-6, and C8-T1 injured subjects experiencing an approximate 65% reduction in cross-sectional area.

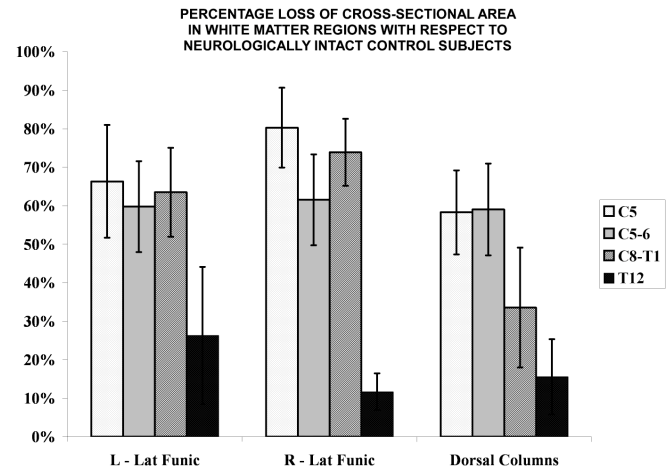


Fig. 3. Percentage loss of cross-sectional area in white matter regions of interest including the left lateral funiculi, right lateral funiculi, and dorsal columns with respect to that of the neurologically intact control subjects.

Diffusion measurements in white matter regions of spinal cord injured subjects indicated a significant decrease in the mean diffusivity for all white matter regions ($p < 0.01$), significant decrease in the transverse apparent diffusion coefficient in the lateral funiculi ($p < 0.001$), and a significant decrease in longitudinal apparent diffusion coefficient in all white matter regions ($p < 0.001$) compared to the neurologically intact control subjects. Longitudinal measured anisotropy (ψ_1) was not significantly lower in the white matter regions for subjects with spinal cord injury ($p = 0.12$) compared to neurologically intact control subjects.

IV. DISCUSSION

Traumatic spinal cord injury can cause significant global changes in the morphology of the spinal cord depending on the severity of injury [12], location of the lesion [13], and the number of target cells the neural fibers involved in the trauma innervate [14]. Previous studies have indicated significant degeneration in the ascending tracts (dorsal columns) and descending tracts (lateral funiculi) occurring after injury as a result of Wallerian degeneration [15]. Our results support this phenomenon. We observed significantly greater retrograde transneuronal degeneration in the lateral tracts in the C5, C5-6, and C8-T1 injured subjects of whom the lesion was on or around the cervical enlargement, compared to the T12 injured subject whom the injury epicenter occurred in the lumbar enlargement. This is consistent with transneuronal degeneration in which lesion sites further away from the imaged site have more probability of existing innervation with noninjured target cells, thus a lower probability of necrosis and lack of degenerative cascading.

Qualitative examination of the neurologically intact control subjects indicated that anisotropy measurements provided a more anatomically accurate representation of internal spinal cord morphology compared to the fractional anisotropy. Primarily, the regions containing the ventral horns in the gray matter were absent in the images of fractional anisotropy but were evident in anisotropy measurements. Analysis of the diffusion coefficients in subjects with spinal cord injury indicated a significant decrease in both longitudinal and transverse diffusion coefficients in regions distal from the injury site. This appears to contradict acute *ex vivo* studies involving animal surrogates that suggest the white matter transverse apparent diffusion coefficient increases following injury [3, 16] and diffusion coefficients in regions distal to the injury epicenter are unaffected [5]. There is, however, evidence in this study to suggest the decrease in transverse diffusion coefficient and overall diffusivity might be due to atrophy of the spinal cord, probably resulting from decreases in axon diameter [7] after degeneration.

No significant differences were found between white matter anisotropy measurements in the injured and control subjects suggesting these metrics may provide a better indication of intact white matter tracts compared to diffusion measurements alone.

V. CONCLUSION

Deficits due to traumatic spinal cord injury can now be assessed via *in vivo* examination of internal cord morphology using diffusion tensor imaging and anisotropy measurements. Fuzzy logic provides an adequate tissue segmentation method for morphometric analysis. Morphometry can then be used to track the progression of degeneration and providing a possible tool for the prediction of neurological functionality based on the measurements of morphological features.

REFERENCES

- [1] E. D. Schwartz, J. T. Duda, J. S. Shumsky, E. T. Cooper, and J. C. Gee, "Spinal cord diffusion tensor imaging and fiber tracking can identify white matter tract disruption and glial scar orientation following lateral funiculotomy," *Journal of Neurotrauma*, vol. 22, pp. 1388-1398, 2005.
- [2] M. J. Shepard and M. B. Bracken, "Magnetic resonance imaging and neurological recovery in acute spinal cord injury: observations from the National Acute Spinal Cord Injury Study 3," *Spinal Cord*, vol. 37, pp. 833-837, 1999.
- [3] J. C. Ford, D. B. Hackney, D. C. Alsop, H. Jara, P. M. Joseph, C. M. Hand, and P. Black, "MRI characterization of diffusion coefficients in a rat spinal cord injury model," *Magnetic Resonance in Medicine*, vol. 31, pp. 488-494, 1994.
- [4] E. D. Schwartz, E. T. Cooper, Y. Fan, A. F. Jawad, C. L. Chin, J. Nissanov, and D. B. Hackney, "MRI diffusion coefficients in spinal cord correlate with axon morphometry," *NeuroReport*, vol. 16, pp. 73-76, 2005.
- [5] E. D. Schwartz, C. L. Chin, J. S. Shumsky, A. F. Jawad, B. K. Brown, S. Wehrli, A. Tessler, M. Murray, and D. B. Hackney, "Apparent Diffusion Coefficients in Spinal Cord Transplants and Surrounding White Matter Correlate with Degree of Axonal Dieback After Injury in Rats," *American Journal of Neuroradiology*, vol. 26, pp. 7-18, 2005.
- [6] B. M. Ellingson, J. L. Ulmer, and B. D. Schmit, "A new technique for imaging the human spinal cord *in vivo*," *Biomed Sci Instrum*, vol. 42, pp. 255-260, 2006.
- [7] J. C. Ford, D. B. Hackney, E. Lavi, M. Phillips, and U. Patel, "Dependence of apparent diffusion coefficients on axonal spacing, membrane premeability, and diffusion time in spinal cord white matter," *Journal of Magnetic Resonance Imaging*, vol. 8, pp. 775-782, 1998.
- [8] J. C. Ford and D. B. Hackney, "Numerical model for calculations of apparent diffusion coefficient (ADC) in permeable cylinders - comparison with measured ADC in spinal cord white matter," *Magn Reson Med*, vol. 37, pp. 387-394, 1997.
- [9] K. Fujiwara, K. Yonenobu, K. Hiroshima, S. Ebara, K. Yamashita, and K. Ono, "Morphometry of the cervical spinal cord and its relation to pathology in cases with compression myelopathy," *SPINE*, vol. 13, pp. 1212-1216, 1988.
- [10] E. H. Mamdani and S. Assilian, "An experiment in linguistic synthesis with a fuzzy logic controller," *International Journal of Man-Machine Studies*, vol. 7, pp. 1-13, 1975.
- [11] A. L. Alexander, K. Hasan, G. Kindlmann, D. L. Parker, and J. S. Tsiruda, "A geometric analysis of diffusion tensor measurements of the human brain," *Magnetic Resonance in Medicine*, vol. 44, pp. 283-91, 2000.
- [12] C. C. Kao, "Chapter 16: Spinal cord cavitation after injury," in *The Spinal Cord and Its Reaction to Traumatic Injury*, W. F. Windle, Ed. New York: Marcel Dekker, 1980, pp. 249 - 270.
- [13] W. F. Windle, "Chapter 5: Cell columns and fiber tracts of the spinal cord," in *The Spinal Cord and Its Reaction to Traumatic Injury*, W. F. Windle, Ed. New York: Marcel Dekker, 1980, pp. 59 - 79.
- [14] O. Steward, "Chapter 24: Reorganization of neural circuitry following central nervous system trauma: Naturally occurring processes and opportunities for therapeutic intervention," in *The Neurobiology of Central Nervous System Trauma*, S. K. Salzman and A. I. Faden, Eds. New York: Oxford, 1994, pp. 266 - 287.
- [15] R. M. Quencer and R. P. Bunge, "The injured spinal cord: Imaging, histopathologic, clinical correlates, and basic science approaches to enhancing neural function after spinal cord injury," *Spine*, vol. 21, pp. 2064-2066, 1996.
- [16] E. D. Schwartz and D. B. Hackney, "Diffusion-weighted MRI and the evaluation of spinal cord axonal integrity following injury and treatment," *Experimental Neurology*, vol. 184, pp. 570-89, 2003.